UNIVERSITY OF BIRMINGHAM

Research at Birmingham

Production of biodegradable foams using supercritical CO2

Kelly, Catherine; Murphy, Shona; Hillerström, A.; Gilling, J.; Massoudi, Sam; Jenkins, Michael; Leeke, Gary

Link to publication on Research at Birmingham portal

Production of Biodegradable Foams Using Supercritical CO_2

C.A. Kelly[a], S.H. Murphy[b], A. Hillerström[c], J. Gilling[d], S. Massoudi[a], M.J. Jenkins[b], G.A. Leeke[a]*

[a]Chemical Engineering, University of Birmingham, Edgbaston, Birmingham. B15 2TT, UK
[b]Metallurgy and Materials, University of Birmingham, Edgbaston, Birmingham, B15 2TT, UK
[c]YKI Institute for Surface Chemistry, Stockholm, 114 86, Sweden
[d]Pera, Nottingham Road, Melton Mowbray, Leicestershire. LE13 0PB, UK

*Corresponding author: g.a.leeke@bham.ac.uk

Abstract

A single screw extrusion process in which CO_2 is injected into the polymer melt has been utilised to produce low density biodegradable poly(DL-lactic acid) ($P_{DL}LA$) foams. High pressure differential scanning calorimetry (DSC) is used to observe the melting point depression of crystalline $P_{DL}LA$ 3051D in the presence of CO_2. In addition, the effect of temperature (110 to 140 °C) and CO_2 pressure (50 to 120 bar) on the viscosity of $P_{DL}LA$ 3051D, in the amorphous and crystalline forms, are investigated through the use of a high pressure rheometer. Foams of $P_{DL}LA$ 3051D are produced in a static environment, under a range of conditions, and these data are utilised to extrude $P_{DL}LA$ 3051D into foamed sheets for packaging applications. The density, crystallinity, mechanical properties and microstructure of these foams are evaluated using DSC, tensile testing and scanning electron microscopy (SEM).

Introduction

Packaging foams are generally produced from synthetic polymers making them hard to recycle. The majority are land-filled following use where they take up a large volume and do not degrade. An alternative approach is to produce foams using biodegradable polymers

obtained from natural sources. At present, only poly(DL-lactic acid) ($P_{DL}LA$) can be produced on a sufficient scale to achieve this, however it is thermally sensitive and often degrades during processing preventing its production into low density foams.[1] Only modified $P_{DL}LA$ has been successfully foamed to a low density (< 50 kg m^{-3}),[2] but this modification also affects the mechanical properties and degradation behaviour.

A solution to this problem is to extrude such polymers in the presence of supercritical CO_2 (scCO_2). Both single and twin screw extruders have been modified to enable CO_2 to be injected into the barrel of the extruder [3-5]. On entering the polymer melt, the gas-like viscosity of CO_2 allows it to diffuse into the amorphous regions whereupon it enters into the free volume between individual chains [6]. Here, it then undergoes Lewis acid/base interactions with the carbonyl groups of PLA weakening the intermolecular interactions between the individual polymer chains [7]. Chain separation increases as a result, enhancing the mobility and thereby reducing the glass transition temperature [8] and viscosity of the polymer [9]. This absorption of CO_2 into amorphous regions is also able to reduce the melting temperature of semi-crystalline polymers. The chemical potential of the amorphous regions is lowered by the absorbed CO_2 which drives the equilibrium towards a less crystalline morphology [10], reducing the melting point of the polymer [11].

In addition to aiding the processing of $P_{DL}LA$, CO_2 can also be used as the foaming agent. On lowering the pressure, the solubility of CO_2 within the polymer is reduced leading to the diffusion of gas into the surroundings. When the CO_2 exits the polymer nucleation occurs resulting in the formation of bubbles. These bubbles grow and coalesce generating the

foamed structure [12]. The removal of CO_2 also causes the glass transition temperature (T_g) and/or melting point (T_m) to rise, solidifying the polymer and fixing the foamed structure. An added advantage is that on exiting the extruder CO_2 returns to the gaseous phase leaving only the pure polymer.

The aim of this work is to evaluate the effect of CO_2 on the glass transition temperature, melting point and viscosity of amorphous and semi-crystalline $P_{DL}LA$ 3051D. These data are then utilised to guide the foaming of $P_{DL}LA$ 3051D in a static vessel and in identifying the optimum processing conditions. Foamed sheets are also produced using a standard extrusion system that has been modified to allow injection of CO_2 into the compression phase of the extruder.

Materials and Methods

Materials

$P_{DL}LA$ (Ingeo^{TM}) 3051D (M_w 134 kDa in chloroform when compared to polystyrene standards) was supplied by Natureworks LLC (Minnetonka, Minnesota). The polymer pellets were dried (as recommended by the supplier) prior to use at 100 °C for 4 hours to ensure the complete removal of moisture. CO_2 (purity 99.995 %v/v) was obtained from BOC (Manchester, UK) and used as received.

Production of Polymer Plaques

Plaques, 250 x 250 mm with a thickness of 0.5 mm, were obtained by compression moulding. Briefly, the dried polymer pellets (7 g) were placed into a mould. The mould was

then inserted into a press, preheated to 200 °C, and a pressure of 10 tonnes applied for 5 minutes. The plaques were removed from the press before being allowed to cool to room temperature. The compression moulding process resulted in an amorphous polymer so, where required, the original crystallinity of $P_{DL}LA$ 3051D was restored by subjecting the plaque to 118 °C for 2 hours.

Crystallinity of $P_{DL}LA$ 3051D

The crystallinity of the polymer plaques and foams were determined by differential scanning calorimetry (DSC) using a HP DSC 827 (Mettler Toledo, Leicester, UK). Briefly, discs (5-10 mg) were cut from the plaques and foams and sealed inside an aluminium DSC pan (Mettler Toledo, Leicester, UK). The sample was then loaded into the DSC at 25 °C and the temperature raised to 180 °C at a rate of 50 °C/min. The weight fraction degree of crystallinity (X_c) was determined from equation 1.

$$Xc = \frac{\Delta H_f(T_m)}{\Delta H_f^0(T_m^0)} \qquad (1)$$

where $\Delta H_f(T_m)$ is the enthalpy of fusion measured at the melting point and $\Delta H_f^0(T_m^0)$ is the enthalpy of fusion of the completely crystalline polymer. A literature value of 93 J g^{-1} was used for $P_{DL}LA$ 3051D [13].

High Pressure Differential Scanning Calorimetry

The effect of supercritical CO_2 on the glass transition temperature and melting point of $P_{DL}LA$ 3051D was investigated using the HP DSC 827. Discs (5-10 mg), were cut from the polymer plaque and sealed inside DSC pans containing lids pierced with 6 pin holes. CO_2 was

charged to the desired pressure and the system left for 1 hour to allow the CO_2 to diffuse into the polymer. Following soaking, the sample was heated from 25 to 180 °C at a rate of 10 °C/min. Previous studies have shown that subjecting semi-crystalline 3051D to $scCO_2$ for 1 hour does not alter its crystallinity (data not shown). The same procedure was followed for studies at atmospheric pressure. The glass transition of $P_{DL}LA$ 3051D often appears with a peak superimposed on it, as a result of relaxations in the polymer, and so the T_g was measured according to the Richardson method [14].

High Pressure Rheology

The effect of temperature and CO_2 pressure on the viscosity of $P_{DL}LA$ 3051D was determined using a Physica MCR 301 rheometer (Anton Paar, Hertford, UK) with a high pressure parallel plate geometry 20 mm in diameter and a 1 mm gap (PP20/pr). Discs, 20 mm in diameter, were cut from both the amorphous and crystalline plaques and two of these discs were inserted into the preheated high pressure cell to fill the gap between the plates. The cell was sealed and charged with CO_2 using a 2600D syringe pump (Teledyne ISCO, Lincoln, NE, USA). The samples were then left for 5 minutes to allow the CO_2 to diffuse into the polymer. In a typical rotational experiment, the shear rate was varied on a log scale from 0.01 to 100 s^{-1} over 2 minutes and data points were recorded every 5 seconds. The actual viscosity of the sample was obtained from the horizontal portion of the trace as this represents the linear viscoelastic region of the polymer.

Static Foaming

A high pressure stainless steel, 60 ml autoclave (Parr Instrument Company, Moline, Illinois) was used to foam $P_{DL}LA$ 3051D. Prior to analysis, the autoclave was heated to the desired temperature. Plates (20 x 20 mm) were cut from both the amorphous and crystalline polymer plaques and three of these, separated by glass wool, were inserted into the autoclave. The autoclave was sealed and charged with CO_2 to generate the desired pressure. After a desired period of time the system was vented through an outlet. The samples were visually inspected for foaming and analysed by scanning electron microscopy (SEM), using a XL30 ESEM TMP (FEI/Philips, Hillsboro, Oregon), and DSC. For the SEM-analysis, the foamed $P_{DL}LA$ 3051D samples were fractured in liquid nitrogen and the cross-sections of the samples analysed. The density was calculated manually from the mass and volume of the sample.

Extrusion

$P_{DL}LA$ 3051D foamed sheets were extruded using a Collins 25 mm single screw extruder (Collins Extrusions Ltd., Bidford-on-Avon, UK), with a L/D ratio of 30, through a 2 x 12 mm strip die. Following extrusion, the sheet was passed over a take-off system where it was cooled by two air jets. CO_2 was added into the compression phase of the screw using a liquid piston pump (model PU-2086 Plus) (Jasco, Essex, UK) fitted with a chiller head to enable CO_2 to be pumped in the liquid form. In a typical experiment, the extruder barrel was heated to the desired temperature. Prior to starting the screw, a constant CO_2 pressure of 190 bar was applied to the barrel to prevent a back flow of polymer into the CO_2 line. Dried semi-crystalline (39±1 % crystallinity) $P_{DL}LA$ 3051D pellets were added to the hopper and the

screw was then set to the required speed. After the polymer had been extruding for 2 minutes, the CO_2 pump was switched to either constant flow or constant pressure mode and the required flow/pressure selected. The CO_2 flow rate was calculated in order to give a set concentration in the extruder compared to the polymer flow. At each condition (temperature, CO_2 flow rate and screw speed) the polymer was extruded for 4 minutes before a sample was taken in order to ensure steady state conditions. The tensile modulus, ultimate tensile strength and strain at break of the resultant foams were determined using a Z030 universal mechanical tester (Zwick/Roell) with a test speed of 10 mm/min. Five samples were analysed for each condition.

Statistical Analysis

Statistical analyses were performed on the rheology data using the student t-test or ANOVA and the least significant difference (LSD) at the 5 % confidence level. Any differences in results were considered significant if the p-value was less then <0.05.

Results and Discussion

Effect of CO_2 on the Thermal Properties of $P_{DL}LA$ 3051D

High pressure DSC studies were performed to determine the effects of $scCO_2$ on the melting point and glass transition temperature of semi-crystalline $P_{DL}LA$ 3051D. Under atmospheric conditions semi-crystalline $P_{DL}LA$ 3051D melts at 152 °C, however the addition of CO_2 decreases this considerably with a 10 °C reduction is observed in the presence of 60 bar CO_2 (Figure 1). The gaseous properties of CO_2 enable it to diffuse into the amorphous regions of

semi-crystalline $P_{DL}LA$ 3051D. Once inside, CO_2 forms Lewis acid/base interactions with the carbonyl groups in the polymer [7]. This disrupts the original intermolecular interactions between the polymer chains, increasing their mobility. The increased movement of the chains also lowers the chemical potential of the amorphous regions, and thereby shifts the equilibrium to a less crystalline state, reducing the melting point of the polymer [15]. Elevating the pressure subsequently increases the amount of CO_2 present, and therefore the concentration absorbed into the polymer [6, 16], enhancing the above effects and further reducing the melting point. A similar depression in the melting point has previously been observed for the semi-crystalline polymers poly(ethylene glycol) [17] and polycaprolactone [18].
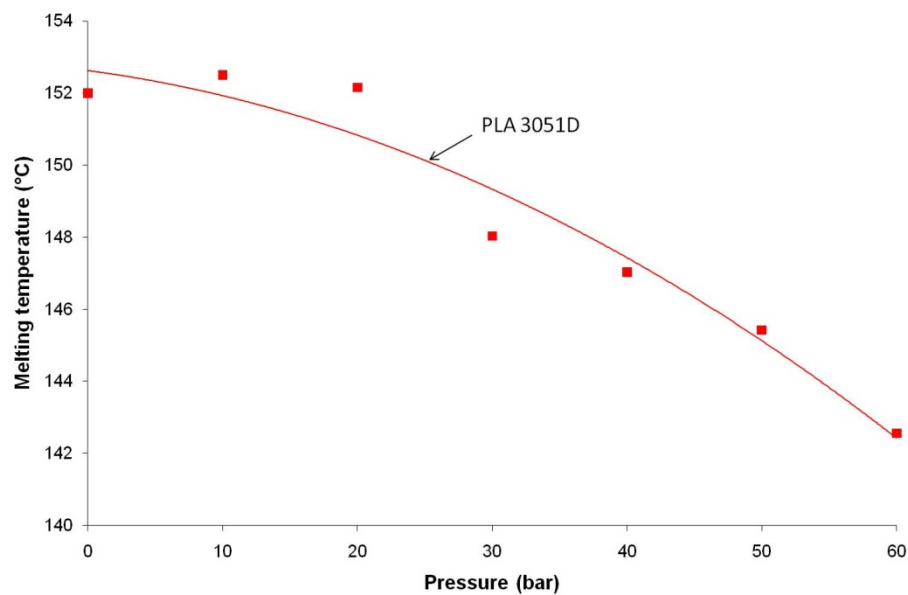

Figure 1: Melting point depression of semi-crystalline $P_{DL}LA$ 3051D with increasing CO_2 pressure as determined by high pressure DSC.

The DSC traces became increasingly noisy as the background pressure increased, due to thermal eddies creating a non-uniform density distribution in the cell, and as a result no

useful data could be obtained above 60 bar. This noise also prevented detection of the glass transition temperature of $P_{DL}LA$ 3051D.

Effect of CO_2 on the Viscosity of $P_{DL}LA$ 3051D

The effect of CO_2 temperature and pressure on the viscosity of $P_{DL}LA$ 3051D was evaluated using a high pressure rheometer with a parallel plate geometry. Results could not be obtained for the crystalline morphology as the melting temperature was above the maximum operation temperature (140 °C) of the rheometer. The amorphous plaques all displayed Newtonian behaviour at low shear rates (0.01 to 1 s^{-1}) followed by shear thinning as the rate was increased (data not shown). This is typical of amorphous polymers as the highly entangled chains become drawn out and aligned during analysis by the rotating motion of the plates [19]. The linear viscoelastic region is plotted for each condition to enable comparisons to be made (Figures 2 and 3).

Rotational tests were performed on the amorphous form of $P_{DL}LA$ 3051D at a range of temperatures (110 to 140 °C) under a fixed pressure of 120 bar. As the temperature of the polymer was increased from 110 to 140 °C; the viscosity subsequently decreased by 97 % (Figure 2). This observation is generally seen with polymers upon heating as more energy is supplied to the material [20-21]. This enhances the mobility of the chains and as a result the viscosity decreases. Previous analyses at ambient pressure have shown the viscosity of semi-crystalline $P_{DL}LA$ (L:D 96:4, Cargill-Dow Polymers) to be reduced by 87 % on raising the temperature from 160 to 200 ºC [22].
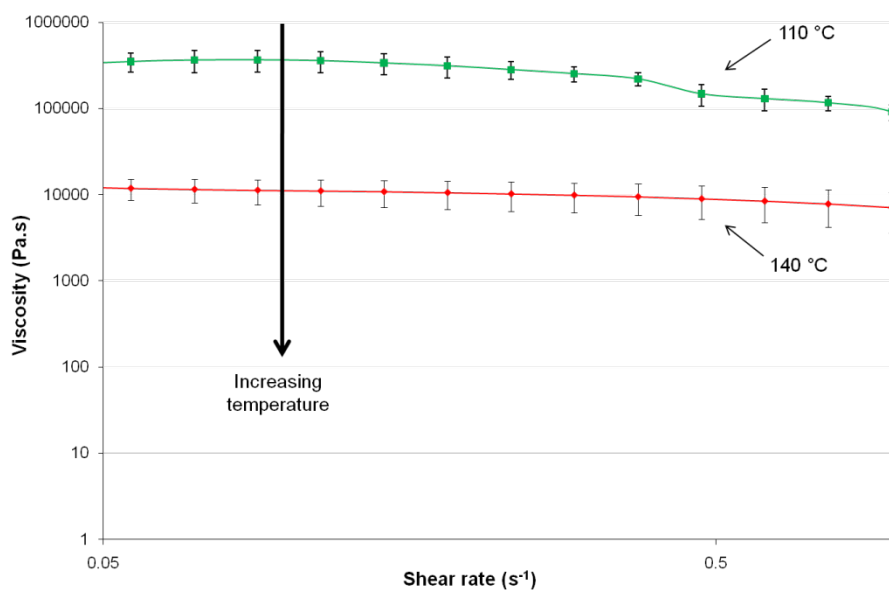
Figure 2: Rheology analysis of amorphous $P_{DL}LA$ 3051D at 120 bar CO_2. Increasing the temperature of the polymer in the presence of CO_2 results in a significant viscosity decrease. p = 0.004

A similar study was undertaken in which the temperature was fixed at 140 °C whilst the pressure was varied (50 to 120 bar). The results (Figure 3) show that as the pressure is increased from 50 to 120 bar the polymer's viscosity significantly decreases. As mentioned above, CO_2 can penetrate into amorphous polymers whereupon it undergoes Lewis acid/base interactions with the chains, weakening their intermolecular interactions [7]. This increases the mobility of the chains thereby reducing the viscosity. As the pressure increases more CO_2 becomes absorbed into the polymer [6] and it therefore follows that the viscosity will be reduced further. A similar trend has been previously observed for $P_{DL}LA$ (M_w 52 kDa, Purac) and $P_{DL}LA$ 2002D (M_w 156 kDa, Natureworks) [21, 23]. However, a reduction in viscosity is not always observed as shown by the significant increase in viscosity at 80 bar (Figure 3). Increasing the system pressure will also increase the pressure surrounding the polymer. This can force the chains back together reducing the effect of the increased CO_2

absorption [24]. These two factors compete against each other to generate the observed viscosity of the polymer.
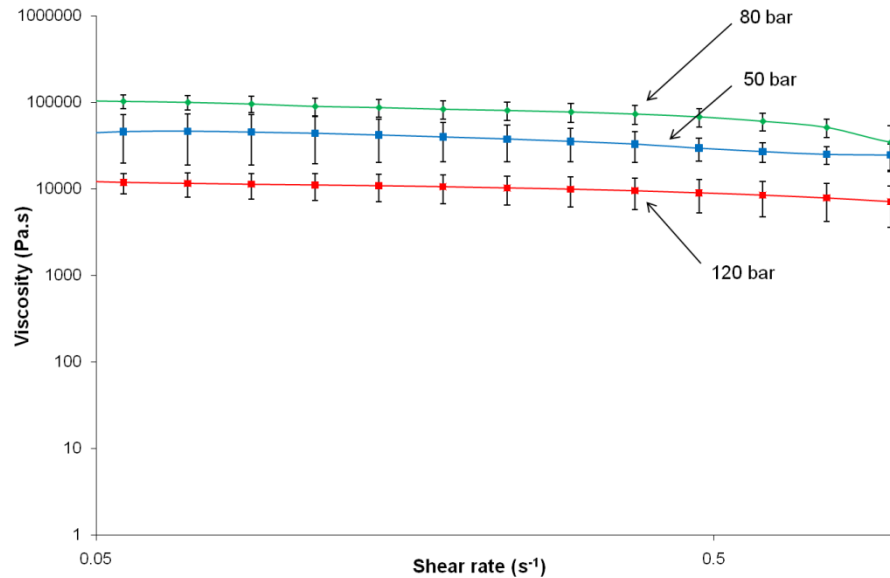
Figure 3: Rheology analysis of amorphous P$_{DL}$LA 3051D at 140 °C. As the pressure is increased from 50 to 120 bar the pressure significantly reduces, however the greatest viscosity is observed at 80 bar. p = 0.005, 5% LSD = 39100 Pa.s.

Foaming of PLA

Thin plates of both semi-crystalline and amorphous P$_{DL}$LA 3051D were subjected to CO_2 at a range of temperatures, pressures and soak times. Foams were then produced following decompression at various vent rates (0.017 − 0.47 L s^{-1}). As mentioned previously, CO_2 is able to diffuse into the amorphous regions of polymers. On decompression, the pressure of the vessel is reduced and concomitantly is the solubility of CO_2 in the polymer. When the CO_2 exits the polymer, nucleation occurs leading to the formation of bubbles. These bubbles grow and coalesce generating the foamed structures [12]. The removal of CO_2 also causes the glass transition temperature and melting point of P$_{DL}$LA 3051D to rise thereby setting the structure of the foam [25].

It was observed that semi-crystalline P_{DL}LA 3051D could not foam under any condition (results not shown). The regular structural array and high density of the intermolecular interactions in crystalline morphologies prevents the diffusion of CO_2 [26], and therefore, absorption only occurs in the amorphous regions of these polymers. As P_{DL}LA 3051D is highly crystalline (approximately 40 %) little CO_2 is absorbed into the polymer plaque, and therefore foaming cannot occur on depressurisation at conditions below its ambient T_m.

Amorphous P_{DL}LA 3051D was foamed using CO_2 at a range of temperatures, pressures, soak times and depressurisation rates (Table 1). It was observed that temperature had a definitive effect on foaming, with foams only being produced at 140 °C. At lower temperatures (70 °C) P_{DL}LA 3051D could not foam, even following soaking for 1 hour. This is likely caused by the high melt strength of the polymer at this temperature preventing expansion of the polymer. Foams were initially observed at 180 °C, however the high temperature, and therefore low viscosity of the polymer, caused the foam to collapse prior to removal from the vessel.

Table 1: Production and analysis of amorphous PLA 3051D foams.

Temperature (°C)	Pressure (bar)	Soak time (min)	Vent rate (L s^{-1})	Result	Density (kg m^{-3})	Crystallinity following foaming (%)
70	150	10	0.07	No foaming	Un-recordable	27.7
70	150	60	0.08	No foaming	Un-recordable	35.0
180	150	10	0.09	Liquefied	Un-recordable	0.0
140	50	2	0.16	Foaming	97	19.9
140	50	5	0.20	Foaming	129	28.8
140	50	10	0.20	Foaming	103	30.3
140	150	2	0.47	Foaming	375	28.4
140	150	2	0.02	Partial foaming	Un-recordable	20.1

At 140 °C, amorphous $P_{DL}LA$ 3051D foams at both 50 and 150 bar although raising the pressure increases the density of the foamed product. At 150 bar, a large pressure will surround the polymer plaque creating a slower, more controlled expansion as the CO_2 is vented. This will lead to a high density compared to the expansion at 50 bar. Lengthening the CO_2 soak time had little effect on both the ability of the material to foam and product density. It is therefore likely that the polymer rapidly reaches it saturation limit, and increasing the soak time has a negligible effect on CO_2 absorption. Another important parameter in the foaming process is the rate at which the CO_2 is vented. The results show that decreasing the vent rate to 0.02 Ls^{-1} prevents foaming, as the CO_2 is able to slowly diffuse out of the polymer hindering the formation of bubbles.

Once in the amorphous form, $P_{DL}LA$ 3051D cannot recrystallise under atmospheric conditions without being subjected to heat for a prolonged period of time [27]. However, the amorphous plaques were observed to crystallise when subjected to CO_2, with the exception of the sample exposed to 180 °C (Table 1). Researchers have previously highlighted the ability of $scCO_2$ to induce crystallisation [28], which was attributed to the mobility of the polymer chains allowing the amorphous regions to rearrange into the more thermodynamically stable crystalline state [29]. This is not observed above the melting point of semi-crystalline $P_{DL}LA$ 3051D as any crystalline regions generated will melt and revert back to the amorphous form following the removal of CO_2. The results show that crystallinity increases with both CO_2 pressure and soak time. A higher CO_2 pressure will result in a greater diffusion into the polymer and therefore a greater mobility of the

polymer chains, allowing further rearrangement to the crystalline state. Also, an increased soak time will create a longer period in which the chains can rearrange, leading to higher crystallinity. A previous study into the CO_2 crystallisation of P_LLA, showing that a 20 % crystallinity could be obtained in under 10 minutes with pressure being a major factor, concurs with these results [30].

Scanning electron microscopy images of two foams are shown in Figure 4. Each of the foams contain a skin which is created by the CO_2 molecules present in the outer layer of the plate diffusing out at a faster rate than nucleation can occur [31]; as a result this layer does not foam. The outer skin enhances the mechanical and barrier properties of the foam producing a material suited to packaging applications.

| 140 °C, 50 bar, 2 min soak | 140 °C, 150 bar, 2 min soak |
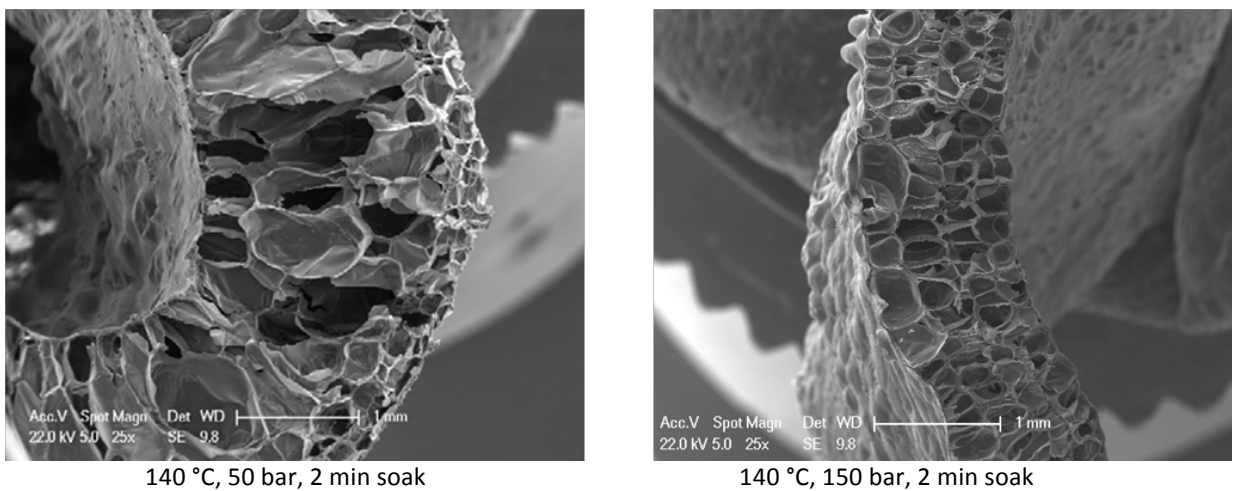
Figure 4: SEM images of amorphous $P_{DL}LA$ 3051D foams produced at various conditions. The foams contained an outer skin which enhances the mechanical and barrier properties of the foam, leading to a suitable packaging material.

Comparison of the SEM images of the foams produced at 50 and 150 bar emphasises the difference in densities calculated previously (Table 1). Visual inspection shows that a more consistent foam, with similar pore sizes, is produced at 150 bar. This is as a result of the

large pressure that surrounds the polymer during the venting process leading to a slower, more controlled expansion of the polymer.

Extrusion of PLA 3051D Foams

A Collins 25mm extruder was modified to allow injection of CO_2 through the barrel and into the compression section of the screw. CO_2 was added as either a constant flow or a constant pressure using the high pressure pump. In constant flow mode, the CO_2 flow rate was adjusted, in relation to the polymer flow rate, to obtain a given CO_2 concentration (0.1-0.5 wt%) in the polymer. Semi-crystalline $P_{DL}LA$ 3051D pellets were extruded over a range of temperatures, CO_2 conditions and screw speeds and the foams analysed to determine the optimum processing conditions. When altering the temperature of the extruder, the barrel prior to the CO_2 inlet remained at 150 °C and only the temperatures of the downstream sections were decreased. This was because in the absence of CO_2 a higher temperature is required for the polymer to flow into the extruder.

Constant Flow Mode

When CO_2 was supplied as a constant flow foams were only produced at specific conditions; however some of the samples that did not foam contained large bubbles (Table 2). These bubbles were created by insufficient mixing of the polymer and CO_2 in the extruder, leading to pockets of undissolved CO_2 in the polymer. As $P_{DL}LA$ 3051D has a high viscosity and melt strength, CO_2 could not easily escape on exiting the die and therefore large bubbles were created. This is particularly evident on reducing the temperature to 140 °C. As the rheological results have shown (Figure 2), reducing the temperature greatly

increases the viscosity of $P_{DL}LA$ 3051D. A higher viscosity will hinder the mixing of the polymer and CO_2 leading to the formation of these bubbles following extrusion. Foam extrusion at temperatures below 140 °C were also attempted but the polymer was too viscous to extrude from the die.

Table 2: Production and analysis of PLA 3051D extruded foams with CO_2 supplied at constant flow.

Temperature (°C)	Screw speed (rpm)	CO_2 concentration (wt%)	Result	Density (kg m^{-3})	Crystallinity (%)
150	5	0.10	Foamed	639	0.2
150	5	0.25	Foamed	518	0.2
150	5	0.50	Bubbles	416	1.1
150	10	0.25	Foamed	355	1.2
150	20	0.25	No foaming	1250	Unrecorded
140	10	0.25	Bubbles	288	0.3

Foams were only produced at low screw speeds (5 and 10 rpm) and CO_2 concentrations (0.1 and 0.25 wt%). During its residence time in the extruder the polymer mixes with the CO_2 molecules, however this mixing process is relatively inefficient due to the high viscosity of $P_{DL}LA$ 3051D and the high polymer pressures experienced inside the barrel. On reaching the die CO_2 nucleates in the polymer leading to the formation of bubbles. The bubbles grow and coalesce generating the foamed structure [12]. At low screw speeds, the residence time in the extruder is increased allowing more time for the CO_2 to diffuse within the polymer chains. This enables a greater absorption of CO_2 into the polymer leading to a greater expansion and therefore foam production when the polymer exits the die.

On increasing the CO_2 concentration two effects are possible: when more CO_2 is present, the amount that penetrates into the polymer is also likely to increase [16], leading to

increased bubble formation on expansion. However, the increase in CO_2 also reduces the viscosity and melt strength, leading to a greater degree of foam collapse on exiting the die. In this case the latter prevails leading to a reduced density on raising the pressure.

$P_{DL}LA$ 3051D did not significantly crystallise during the extrusion process resulting in an amorphous product. This conflicts with the crystallinity data obtained from the foams produced in the high pressure stainless steel autoclave. As discussed previously, the dissolution of CO_2 into the polymer increases the chain separation thereby enhancing mobility. This allows the chains to realign to the more thermodynamically stable crystalline state. However, during extrusion, the polymer is being conveyed through the barrel and so this rearrangement is hindered due to shear forces, leading to very little crystallinity.

SEM analysis on the extruded foams reveals an inhomogeneous structure containing small bubbles on the bottom and larger pores in the middle (Figure 5). On leaving the die, two processes occur to generate the foamed structure: bubble nucleation and bubble growth. At the bottom of the foam these two processes occur at a similar rate leading to the formation of small pores. However, the release of CO_2 from the polymer core is hindered by the additional path length and therefore fewer nucleation sites are formed. Simultaneously, the bubble growth continues leading to the formation of fewer, larger bubbles.
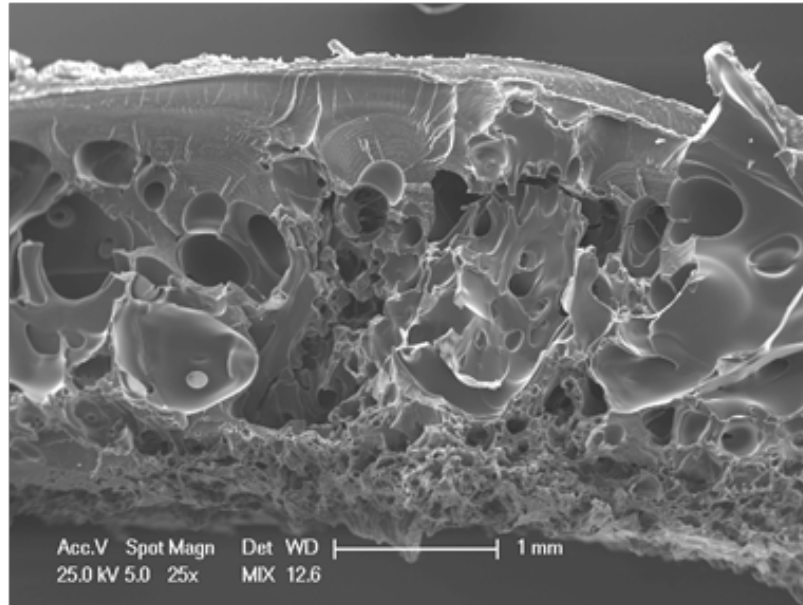
Figure 5: P$_{DL}$LA 3051D foam extruded at 150 °C with a screw speed of 5 rpm and a CO$_2$ concentration of 0.25 %. An inconsistent foaming profile is obtained.

Constant Pressure

Foams were produced when CO$_2$ was supplied at constant pressure for the majority of the conditions studied (Table 5). At both 5 and 20 rpm there was insufficient mixing between the polymer and CO$_2$ causing an irregular polymer flow and large oscillations in the barrel pressure. As a result, the CO$_2$ pressure could not be maintained and therefore no pressure was recorded at these screw speeds.

Table 3: Production and analysis of PLA 3051D extruded foams with CO$_2$ supplied at constant pressure.

Temperature (°C)	Screw speed (rpm)	Pressure (bar)	Result	Density (kg m^{-3})	Crystallinity (%)
140	5	Un-recordable	Foamed	585	1.0
140	10	50	Foamed	477	1.0
140	10	80	Foamed	393	1.3
140	10	120	Foamed	729	3.1
140	20	Un-recordable	No foaming	1124	1.4

It can be seen that low to moderate screw speeds are required to produce foams due to the increased residence time in the extruder, which would enable greater potential for CO$_2$

absorption into the polymer. This study also reveals that the density of the foam is inversely proportional to the viscosity of the polymer (see Figure 3 for viscosity data). On exiting the die the higher viscosity will hinder the loss of CO_2 resulting in greater bubble growth and therefore a more foamed structure.

SEM analysis of the extruded foams reveals an inhomogeneous structure containing a core of large bubbles surrounded by smaller ones (Figure 6). As mentioned above, on leaving the die both bubble nucleation and bubble growth occur simultaneously. Again, at the edges these two processes occur at a similar rate leading to the formation of small pores; whilst the release of CO_2 from the core is hindered resulting in fewer nucleation sites and a large bubble growth.
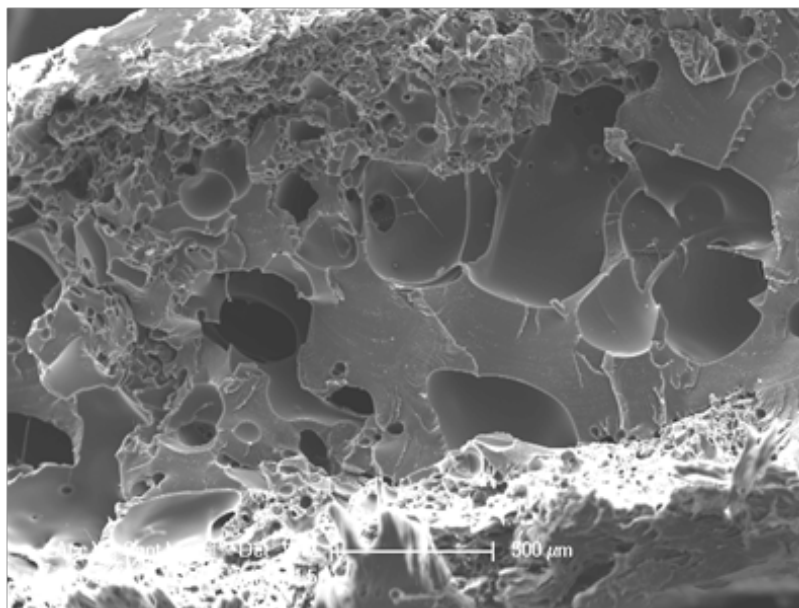

Figure 6: P$_{DL}$LA 3051D foam extruded at 140 °C and 50 bar with a screw speed of 10 rpm. An inconsistent foaming profile is obtained.

Mechanical Properties of Extruded Foams

The mechanical properties of the $P_{DL}LA$ 3051D foams extruded when CO_2 is supplied as a constant flow were analysed. The results (Table 4) show a clear rise in the Young's modulus and ultimate tensile strength on increasing the temperature of the extruder, which is consistent with an increase in the density of the material. Increasing the screw speed of the extruder from 5 to 10 rpm resulted in a reduction in the magnitude of both mechanical properties which is again in line with a reduced density, however this trend was not repeated at 20 rpm. At 20 rpm the material was unable to foam and as a result the density was equivalent to that of unprocessed $P_{DL}LA$ 3051D, This gives rise to the high mechanical properties observed. Varying the quantity of CO_2 injected into the polymer produced little effect on the Young's modulus and ultimate tensile strength of the foams created however, it considerably reduced the strain at break.

Table 4: Mechanical properties of extruded foams produced with CO_2 supplied as a constant flow. Five foams were analysed for each condition.

Temperature (°C)	Screw speed (rpm)	CO_2 concentration (wt%)	Density (kg m^{-3})	Young's modulus (MPa)	Ultimate tensile strength (MPa)	Strain at break (%)
150	5	0.1	639	478	11.8	5.0
150	5	0.25	518	669	15.8	4.0
150	5	0.5	416	504	11.4	3.3
150	10	0.25	355	424	12.6	4.9
150	20	0.25	1250	1551	55.5	6.9
140	10	0.25	288	192	4.7	4.6
Expandable polystyrene tray			52	30	1.2	5.4

Comparison of the mechanical properties of the $P_{DL}LA$ foamed sheets with a commercially available expandable polystyrene (EPS) tray showed a much greater Young's modulus and ultimate tensile stress as a result of the increased density. This provides strength within the

material and therefore, on reducing the density of $P_{DL}LA$ 3051D further, the mechanical properties will approach those of EPS.

Conclusions

The ability of $scCO_2$ to reduce the melting point and viscosity of semi-crystalline and amorphous $P_{DL}LA$ 3051D has been investigated and this knowledge applied to enable the production of foams in a static environment at temperatures as low as 140 °C.

A single screw extrusion process, modified to enable the injection of CO_2 into the compression phase of the extruder, has been successfully utilised to foam $P_{DL}LA$ 3051D at 60 °C below its standard processing temperature thereby preventing degradation. These foams have densities as low as 288 kg m^{-3} and displayed suitable mechanical properties for packaging applications. The use of CO_2 as a processing aid and foaming agent replaces the need for additives thereby producing a pure, biodegradable product that can be used in food packaging.

Acknowledgments

References

1. Nishida, H., *Thermal degradation*, in *Poly(lactic acid) Synthesis, Structures, Properties, Processing and Application*, R. Auras, et al., Editors. 2010, John Wiley and Sons: Hoboken, NJ. p. 401.

2. Cink, K., et al., *Extruded polylactide foams blown with carbon dioxide. Patent WO 2005/097878* 2005.

3. Alavi, S. and S.S.H. Rizvi, *Strategies for enhancing expansion in starch-based microcellular foams produced by supercritical fluid extrusion.* International Journal of Food Properties, 2005. **8**(1): p. 23-34.

4. Verreck, G., et al., *The effect of pressurized carbon dioxide as a plasticizer and foaming agent on the hot melt extrusion process and extrudate properties of pharmaceutical polymers.* Journal of Supercritical Fluids, 2006. **38**(3): p. 383-391.

5. Wilding, M.D. and D.G. Baird, *Melt Processing and Rheology of an Acrylonitrile Copolymer With Absorbed Carbon Dioxide.* Polymer Engineering and Science, 2009. **49**(10): p. 1990-2004.

6. Pini, R., et al., *Sorption and swelling of poly(DL-lactic acid) and poly(lactic-co-glycolic acid) in supercritical CO2: An experimental and modeling study.* Journal of Polymer Science Part B-Polymer Physics, 2008. **46**(5): p. 483-496.

7. Kazarian, S.G., et al., *Specific intermolecular interaction of carbon dioxide with polymers.* Journal of the American Chemical Society, 1996. **118**(7): p. 1729-1736.

8. Kikic, I., et al., *Polymer plasticization using supercritical carbon dioxide: Experiment and modeling.* Industrial & Engineering Chemistry Research, 2003. **42**(13): p. 3022-3029.

9. Gourgouillon, D., et al., *Simultaneous viscosity and density measurement of supercritical CO2-saturated PEG 400.* Journal of Supercritical Fluids, 1998. **13**(1-3): p. 177-185.

10. Shenoy, S.L., T. Fujiwara, and K.J. Wynne, *Quantifying supercritical CO2 dilation of poly(vinylidene fluoride) and poly(vinylidene fluoride-co-hexafluoro-propylene) utilizing a linear variable differential transducer: Plasticization and melting behavior.* Macromolecular Symposia, 2003. **201**: p. 171-178.

11. Madsen, L.A., *Plasticization of poly(ethylene oxide) in fluid CO2 measured by in-situ NMR.* Macromolecules, 2006. **39**(4): p. 1483-1487.

12. Davies, O.R., et al., *Applications of supercritical CO2 in the fabrication of polymer systems for drug delivery and tissue engineering.* Advanced Drug Delivery Reviews, 2008. **60**(3): p. 373-387.

13. Ahmed, J., et al., *Thermal properties of polylactides: Effect of molecular mass and nature of lactide isomer.* Journal of Thermal Analysis and Calorimetry, 2009. **95**(3): p. 957-964.

14. Aras, L. and M.J. Richardson, *The glass-transition behavior and thermodynamic properties of amorphous polystyrene.* Polymer, 1989. **30**(12): p. 2246-2252.

15. Lian, Z.Y., et al., *Carbon dioxide-induced melting point depression of biodegradable semicrystalline polymers.* Journal of Supercritical Fluids, 2006. **39**(1): p. 107-117.

16. Leeke, G.A., J.G. Cai, and M. Jenkins, *Solubility of supercritical carbon dioxide in polycaprolactone (CAPA 6800) at 313 and 333 K.* Journal of Chemical and Engineering Data, 2006. **51**(5): p. 1877-1879.

17. Weidner, E., et al., *Phase equilibrium (solid-liquid-gas) in polyethyleneglycol-carbon dioxide systems.* Journal of Supercritical Fluids, 1997. **10**(3): p. 139-147.

18. Kelly, C.A., et al., *Detection of Melting Point Depression and Crystallisation of Polycaprolactone (PCL) in scCO2 by FTIR.* Accepted to Polymer Journal

19. Palade, L.I., H.J. Lehermeier, and J.R. Dorgan, *Melt rheology of high L-content poly(lactic acid).* Macromolecules, 2001. **34**(5): p. 1384-1390.

20. Mavridis, H. and R.N. Shroff, *Temperature dependence of polyolefin melt rheology.* Polymer Engineering and Science, 1992. **32**(23): p. 1778-1791.

21. Kelly, C.A., et al., *Viscosity studies of poly(DL-lactic acid) in supercritical CO2.* Journal of Polymer Science Part B: Polymer Physics, 2012. **50**(19): p. 1383-1393.

22. Lehermeier, H.J. and J.R. Dorgan, *Melt rheology of poly(lactic acid): Consequences of blending chain architectures.* Polymer Engineering and Science, 2001. **41**(12): p. 2172-2184.

23. Tai, H., et al., *Studies on the interactions of CO(2) with biodegradable poly(DL-lactic acid) and poly(lactic acid-co-glycolic acid) copolymers using high pressure ATR-IR and high pressure rheology.* Polymer, 2010. **51**(6): p. 1425-1431.

24. Nalawade, S.P., et al., *Prediction of the viscosity reduction due to dissolved CO2 of and an elementary approach in the supercritical CO2 assisted continuous particle production of a polyester resin.* Powder Technology, 2006. **170**(3): p. 143-152.

25. Shieh, Y.T., et al., *Interaction of supercritical carbon dioxide with polymers .2. Amorphous polymers.* Journal of Applied Polymer Science, 1996. **59**(4): p. 707-717.

26. Shieh, Y.T., et al., *Interaction of supercritical carbon dioxide with polymers .1. Crystalline polymers.* Journal of Applied Polymer Science, 1996. **59**(4): p. 695-705.

27. Bigg, D.M., *Polylactide copolymers: Effect of copolymer ratio and end capping on their properties.* Advances in Polymer Technology, 2005. **24**(2): p. 69-82.

28. Liao, X., et al., *Effect of supercritical carbon dioxide on the crystallization and melting behavior of linear bisphenol A polycarbonate.* Journal of Polymer Science Part B-Polymer Physics, 2004. **42**(2): p. 280-285.

29. Beckman, E. and R.S. Porter, *Crystallisation of bisphenol A polycarbonate induced by supercritical carbon dioxide.* Journal of Polymer Science Part B-Polymer Physics, 1987. **25**(7): p. 1511-1517.

30. Alessi, P., et al., *Plasticization of polymers with supercritical carbon dioxide: Experimental determination of glass-transition temperatures.* Journal of Applied Polymer Science, 2003. **88**(9): p. 2189-2193.

31. Goel, S.K. and E.J. Beckman, *Generation of microcellular polymeric foams using supercritical carbon dioxide. II: Cell growth and skin formation.* Polymer Engineering & Science, 1994. **34**(14): p. 1148-1156.